

International Journal of Hyperthermia



ISSN: (Print) (Online) Journal homepage: www.tandfonline.com/journals/ihyt20

Combination cancer imaging and phototherapy mediated by membrane-wrapped nanoparticles

Sara B. Aboeleneen, Mackenzie A. Scully, George C. Kramarenko & Emily S. Day

To cite this article: Sara B. Aboeleneen, Mackenzie A. Scully, George C. Kramarenko & Emily S. Day (2023) Combination cancer imaging and phototherapy mediated by membrane-wrapped nanoparticles, International Journal of Hyperthermia, 40:1, 2272066, DOI: 10.1080/02656736.2023.2272066

To link to this article: https://doi.org/10.1080/02656736.2023.2272066

<u>a</u>	© 2023 The Author(s). Published with license by Taylor & Francis Group, LLC
	Published online: 30 Oct 2023.
	Submit your article to this journal 🗗
hil	Article views: 1027
Q	View related articles 🗹
CrossMark	View Crossmark data ☑





Combination cancer imaging and phototherapy mediated by membranewrapped nanoparticles

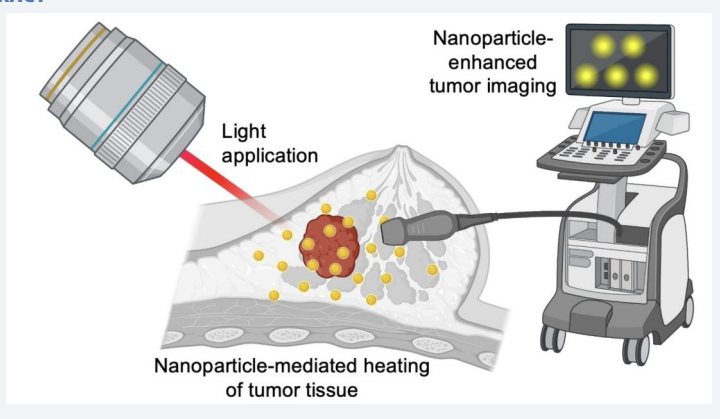
Sara B. Aboeleneen^{a*} (D), Mackenzie A. Scully^{a*} (D), George C. Kramarenko^a (D) and Emily S. Day^{a,b,c} (D)

^aDepartment of Biomedical Engineering, University of Delaware, Newark, DE, USA; ^bDepartment of Materials Science & Engineering, University of Delaware, Newark, DE, USA; ^cHelen F. Graham Cancer Center & Research Institute, Newark, DE, USA

ABSTRACT

Cancer is a devastating health problem with inadequate treatment options. Many conventional treatments for solid-tumor cancers lack tumor specificity, which results in low efficacy and off-target damage to healthy tissues. Nanoparticle (NP)-mediated photothermal therapy (PTT) is a promising minimally invasive treatment for solid-tumor cancers that has entered clinical trials. Traditionally, NPs used for PTT are coated with passivating agents and/or targeting ligands, but alternative coatings are being explored to enhance tumor specific delivery. In particular, cell-derived membranes have emerged as promising coatings that improve the biointerfacing of photoactive NPs, which reduces their immune recognition, prolongs their systemic circulation and increases their tumor accumulation, allowing for more effective PTT. To maximize treatment success, membrane-wrapped nanoparticles (MWNPs) that enable dual tumor imaging and PTT are being explored. These multifunctional theranostic NPs can be used to enhance tumor detection and/or ensure a sufficient quantity of NPs that have arrived in the tumor prior to laser irradiation. This review summarizes the current state-of-the-art in engineering MWNPs for combination cancer imaging and PTT and discusses considerations for the path toward clinical translation.

GRAPHICAL ABSTRACT



ARTICLE HISTORY

Received 21 July 2023 Revised 10 October 2023 Accepted 11 October 2023

KEYWORDS

Biomimicry; photothermal therapy; theranostic; multimodal imaging; nanomedicine; hyperthermia

1. Introduction

1.1. Overview of nanoparticle-mediated photothermal therapy and imaging for cancer management

Cancer is a global health problem that lacks effective treatments despite tremendous efforts to identify cures. It is the second leading cause of death in the United States where in 2023 alone there will be approximately two million new cases and over 600,000 expected deaths [1]. Conventional treatments for solid-tumor cancers include surgical resection, radiotherapy and chemotherapy, applied

alone or in combination. Surgery is most beneficial in early disease stages before metastasis has occurred and failure to resect all cancer cells can lead to recurrence. Additionally, surgical trauma can induce inflammation that promotes metastasis [2], so surgery is typically combined with chemotherapy or radiotherapy. Unfortunately, radiotherapy and chemotherapy also have limitations, such as causing unintentional harm to healthy tissues or having limited therapeutic effect owing to cellular resistance mechanisms [3]. Due to these limitations, researchers have been exploring alternative treatment approaches, including

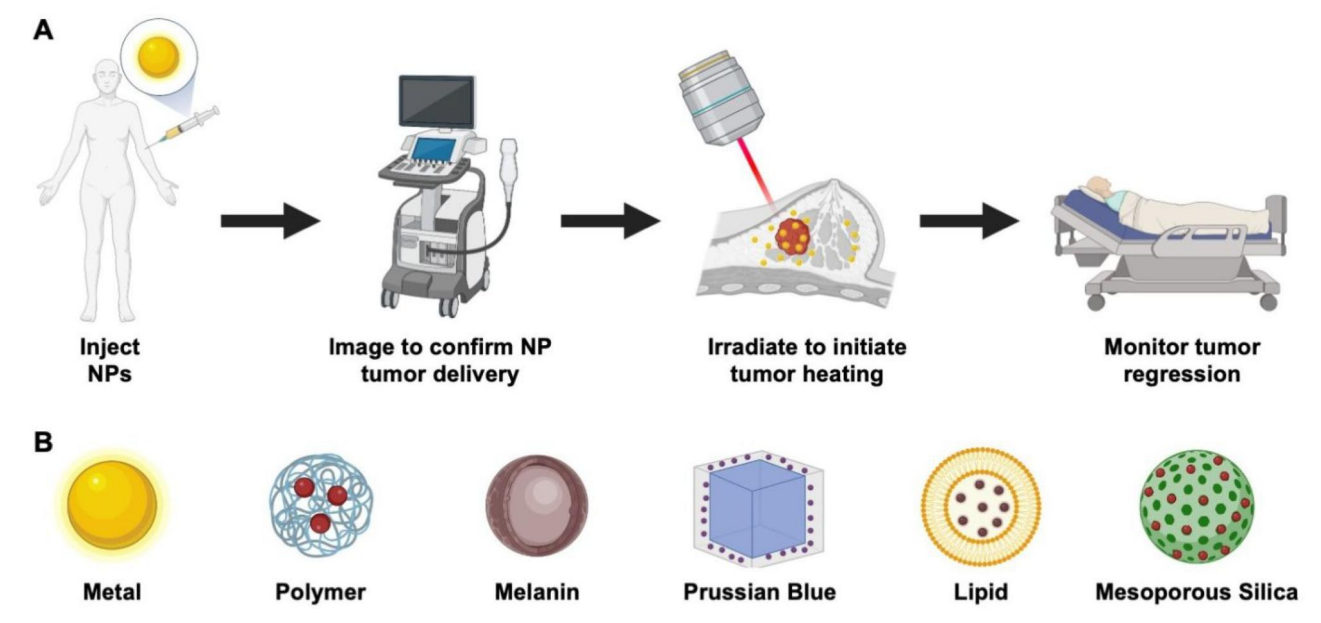
the application of photothermal therapy (PTT) mediated by nanoparticles (NPs).

PTT is a minimally invasive, high precision treatment that uses light-sensitive NPs as exogenous energy absorbers to convert incident light into heat that irreversibly damages tumors. The light-sensitive NPs are administered intravenously (IV) and accumulate in the tumor, which is then irradiated with an externally applied laser tuned to match the peak absorbance wavelength of the NPs [4]. Near-infrared (NIR) light (spanning 650–900 nm) is most often used because it penetrates tissue more deeply than wavelengths outside this range. Excitingly, PTT mediated by silica core/gold shell nanoshells has entered human clinical trials with promising results, warranting further investigation of NP-mediated PTT as a viable treatment for solid-tumor cancers [5–7].

Many NPs used for PTT can enable dual imaging and therapy. Materials that support both diagnostic imaging and treatment are known as 'theranostics' and can facilitate image-guided cancer therapy (Scheme 1A). Various theranostic NPs have been explored pre-clinically for the dual imaging and PTT of solid tumors. These include NPs loaded with NIR dyes (such as indocyanine green (ICG) [8-11], IR780 [12], IR792 [13] and IR1048 [14]), semiconducting polymer NPs [15,16], gold NPs [17,18], iron oxide NPs [19-22], melanin NPs [23,24] and others (Scheme 1B) [25-29]. While dyeloaded polymeric NPs, lipid NPs and mesoporous silica NPs rely on the light-absorbing properties of the encapsulated dye to achieve their phototherapeutic and/or imaging capabilities, other NPs such as those based on gold, Prussian blue or melanin exploit the optical/plasmonic properties inherent to the material. The features of these materials will be discussed, compared and contrasted more throughout this review, but the key advantage of theranostics generally is that they can guide and assess PTT in real-time, for instance,

by ensuring sufficient NP accumulation within the tumor prior to light application, thus improving therapeutic effect. If implemented successfully, this would allow clinicians to tune laser fluence, irradiation time and/or the dose of administered NPs for each individual patient to maximize tumor response [30].

For IV-administered theranostic NPs to accumulate within tumors, they must first safely navigate the blood where they are exposed to various serum and opsonin proteins that can tag them as foreign bodies, altering their biological identity and signaling their rapid clearance by the mononuclear phagocytic system (MPS) [31]. If the NPs are degraded or excreted too quickly from the body or become trapped in healthy tissues, their concentration in the tumor will not be high enough to produce adequate heat upon laser irradiation to cause cancer cell death. Accordingly, understanding and controlling the protein corona that forms around NPs after IV injection is imperative to their success. The protein corona has been reviewed in detail elsewhere [32,33], but it consists of both a 'hard' inner layer of proteins with high affinity for the NP surface and a 'soft' outer layer of proteins with lower affinity for the NP surface. The protein corona (particularly the soft corona) is dynamic, and the composition will change based on the physicochemical properties of the NP, including any surface coatings [34]. To minimize protein adsorption and immune clearance, NPs are usually coated with neutral polymers like poly(ethylene glycol) (PEG), which reduces opsonization, prolongs circulation and increases passive tumor accumulation. However, PEGylated NPs can cause an anti-PEG immune response, do not solve sequestration problems by the MPS organs and do not provide active targeting of cancer cells, so researchers are developing alternative coatings with better immune evasion and targeting capabilities [35,36].

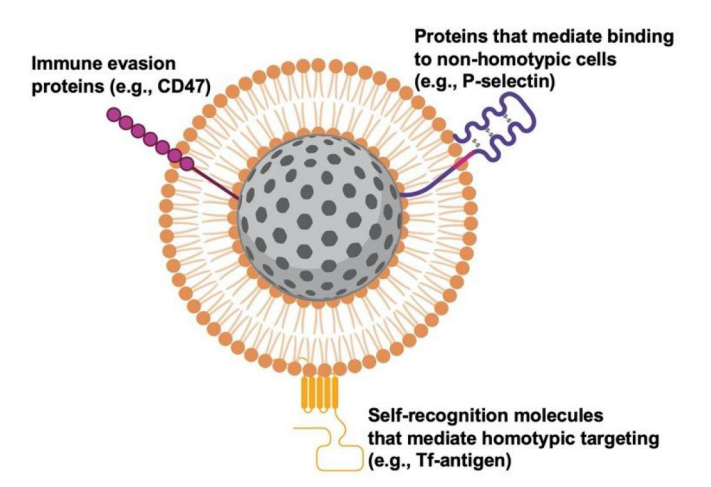


Scheme 1. Overview of theranostic NPs for dual cancer imaging and PTT. (A) Depiction of the process to use NPs for real-time imaging to guide PTT. (B) Summary of various NP formulations that have used pre-clinically as phototheranostics. Red spheres in the polymer, lipid and silica formulations indicate encapsulated light-responsive dyes. Created with BioRender.com.

1.2. Cell membrane wrapping to maximize NP tumor delivery

To target cancer cells more precisely, NPs can be coated with moieties like antibodies, peptides, aptamers or other ligands that selectively bind receptors that are overexpressed on the cancer cell surface [37]. However, this strategy has only modestly improved tumor delivery of NPs [37,38]. This is in part because cancer cells exhibit heterogenous receptor expression, so targeting a single molecule is insufficient [37]. Additionally, the ligand density must be properly tuned or the NPs will exhibit insufficient binding to target cells and potentially off-target binding to perivascular cells before they can penetrate deeply into the tumor [38]. To overcome these challenges of ligand-targeted NPs, researchers have turned to biomimicry as a promising biointerfacing strategy.

The general concept of biomimicry is to coat NPs with cell-derived biological membranes, which imparts the NPs with exceptional biointerfacing capabilities owing to the unique combination of proteins, receptors and phospholipids present in the membrane. These molecules facilitate both immune evasion and cellular binding capabilities, which together enhance the tumor accumulation of membranewrapped nanoparticles (MWNPs) compared to their uncoated counterparts (Scheme 2). This idea was first popularized by Zhang and colleagues, who showed that poly(lactic-co-glycolic acid) (PLGA) NPs wrapped with red blood cell (RBC) membranes exhibited a circulation half-life of 39.6 h versus a 15.8 h half-life for their PEGylated counterpart [39]. This extended circulation time was attributed to the presence of CD47 'marker of self' proteins on the RBC membranes that reduced NP phagocytosis by immune cells [39]. These remarkable results encouraged an explosion of research into the use of cell-derived membranes as NP coatings to enhance drug delivery, gene regulation, PTT, imaging and other applications [40-43]. Membranes from numerous cell types have been explored, including platelets, fibroblasts, leukocytes, cancer cells, stem cells, immune cells, bacteria and others. The advantages and disadvantages of different membrane sources have recently been reviewed [42]. The



Scheme 2. Cell-derived membranes include distinct molecules that facilitate immune evasion, enable binding to non-homotypic cells or promote binding to homotypic cells. Together, these features enhance the tumor accumulation of MWNPs. Created with BioRender.com.

choice of which cell type to use as the membrane source largely depends on the specific tissue/disease to be targeted, since the targeting ability of MWNPs relies on the specific transmembrane proteins present in the membrane coating. Some proteins can mediate binding to non-homotypic cells, such as P-selectin which allows platelets (and platelet MWNPs) to bind CD44 receptors on cancer cells (Scheme 2) [14]. Other 'self-recognition' proteins allow for homotypic targeting of cells that match the membrane source. For instance, Thomsen-Friedenreich antigen (Tf-antigen) interacts with galectins on cancer cells to promote tumor cell aggregation and metastasis, and hence cancer cell MWNPs that incorporate Tf-antigen can demonstrate homotypic targeting (Scheme 2) [44,45]. While more work is needed to fully elucidate which proteins mediate the immune evasion and targeting capabilities of MWNPs, they are clearly critical for the unique biointerfacing properties of these materials.

The synthetic routes to produce MWNPs have previously been reviewed [40], but in brief the steps include (1) membrane extraction from source cells, (2) fabrication of the NP core and (3) surrounding the NPs with the membranes to form MWNPs. Membrane extraction techniques include freeze-thaw cycling, electroporation and lysis coupled with homogenization [40]. Once collected, membranes can be coated onto NPs by sonication, microfluidic mixing or extrusion techniques [40]. Post-synthesis, it is important that MWNPs be carefully characterized for their size, zeta potential and membrane protein content and completeness [40], as recent work has shown cell membrane coating integrity affects the biological fate of MWNPs [46]. It is also critical to characterize the optical properties of MWNPs intended for use in PTT and imaging applications. The following portions of this review summarize the current state-of-the-art in the use of MWNPs for combined cancer imaging and PTT and provide insight to the path forward for clinical translation. A list of abbreviations used in the review is provided in Table 1 to assist readers.

2. Membrane-wrapped NPs for dual PTT/imaging of solid-tumor cancers

Owing to the improved biointerfacing capabilities of MWNPs that increase their tumor accumulation, researchers are now exploring these tools for dual tumor imaging and PTT. Various imaging techniques have been used to monitor the tumor accumulation of MWNPs and thereby guide PTT, including photoacoustic (PA) imaging, magnetic resonance imaging (MRI), fluorescence (FL) imaging and other modalities. These are introduced briefly below and compared in Table 2, followed by in-depth discussion of the MWNPs that have been developed for use with each modality.

PA imaging is a noninvasive, high-resolution technique that uses photothermally converted acoustic waves to realize ultrasound signal detection [16,17]. That is, when photothermally active NPs within tissue are excited with pulsed NIR light, the produced heat leads to thermal tissue expansion and generation of an acoustic pressure wave that can be detected by an ultrasound transducer. Because PA imaging



Table 1. List of common abbreviations found throughout this review.

Abbreviation	Expanded term	Abbreviation	Expanded term
AF	Activated fibroblast	MPS	Mononuclear phagocytic system
BBB	Blood-brain barrier	MRI	Magnetic resonance imaging
BTB	Blood-tumor barrier	MSC	Mesenchymal stem cell
CT	Computed tomography	MWNP(s)	Membrane-wrapped nanoparticle(s)
CW	Continuous wave	NIR	Near-infrared
DOX	Doxorubicin	NP(s)	Nanoparticle(s)
DTX	Docetaxel	PA	Photoacoustic
Ex	Excitation	PDT	Photodynamic therapy
Em	Emission	PEG	Poly(ethylene glycol)
FA	Folic acid	PLGA	Poly(lactic-co-glycolic acid)
FL	Fluorescence	PTT	Photothermal therapy
HSP	Heat shock protein	RBC	Red blood cell
HU	Hounsfield unit	SERS	Surface-enhanced Raman scattering
ICG	Indocyanine green	siRNA	Small interfering ribonucleic acid
IV	Intravenous	SNR	Signal-to-noise ratio
Luc	Luciferase	SPN(s)	Semiconducting polymer nanoparticle(s)
MDSC	Myeloid-derived suppressor cell	TPP	Triphenylphosphine
MNC	Magnetic nanocluster		

Other abbreviations such as those for specific MWNP formulations are defined where called out in the text.

Table 2. Comparison of different imaging modalities that have been utilized in combination with phototheranostic NPs.

Imaging modality	Excitation source	Tissue penetration depth	Resolution	Pros	Cons
PA imaging	Light	10 mm–9 cm	30–700 μm	High resolutionHigh tissue penetrationFast acquisition	Small imaging surface area
MRI	Magnetic field	>10 cm	50 μm–2 mm	 High resolution Large imaging surface area 	Low sensitivitySlow acquisition
FL imaging	Light	1–20 mm	1–500 μm	High resolutionFast acquisition	Low tissue penetration
CT	X-ray	>10 cm	50 μm–1 mm	High resolutionHigh relative speed	Radiation exposure
SERS imaging	Light	5–25 mm	<1 μm	High sensitivityHigh photostability	Limited tissue penetrationLow relative speed

detects phonons rather than photons under light excitation, it has superior penetration depth compared to typical FL imaging, along with enhanced spatial resolution and high contrast [16,17]. PA imaging can also provide information about tissue oxygenation and hemodynamics, but a drawback is that only a small area of the body can be imaged at once [47]. By comparison, MRI can image large areas of the body and offers unparalleled spatial resolution. However, MRI has lower sensitivity and data acquisition can be time-consuming and uncomfortable for subjects [47]. In MRI, an applied magnetic field aligns protons within the body. Short bursts of radiofrequency energy are applied, which alters the protons' alignment. When the pulse stops, the protons realign with the magnetic field, releasing electromagnetic energy that is detected and reconstructed into images that distinguish tissues based on the speed of relaxation. Different types of contrast can be achieved with MRI, including T1-weighted imaging (related to spin-lattice relaxation) and T2-weighted imaging (related to spin-spin relaxation). Magnetic NPs can increase contrast by shortening T1 and T2 relaxation. The most common contrast agents are based on iron oxide NPs, which provide negative (dark) contrast in T2weighted images, although other materials such as those based on lanthanide metals can provide positive (bright) contrast in T1-weighted images [48].

FL imaging is commonly used in nanomedicine research as many NPs are inherently fluorescent or can be tagged with fluorescent dyes. FL imaging provides fast real-time scanning but has poor depth penetration [43]. Traditionally,

the absorption and emission wavelengths of NPs used for PTT and FL imaging exist in the first NIR (NIR-I) window (650–950 nm). More recently, NPs that strongly absorb/emit light in the second NIR window (1000-1700 nm) have been developed for NIR-II FL imaging [14]. Compared to NIR-I, NIR-II FL imaging can penetrate deeper into tissue and has lower autofluorescence and higher signal-to-noise ratio (SNR) owing to less light scattering and absorption in biological tissues [13]. The safety threshold of lasers in biological tissues is also improved in the second NIR window, which may promote clinical acceptance of NPs that absorb light in this range for precision cancer imaging and therapy [13]. An important consideration for FL imaging (as well as PA imaging) is the difference between continuous wave (CW) and pulsed lasers. CW lasers emit an uninterrupted beam of light with constant energy output over time, whereas pulsed lasers emit light in short, high-energy bursts with defined pulse durations and intervals. Pulsed lasers are used in techniques such as PA imaging and multiphoton microscopy, whereas CW lasers are used in traditional FL imaging. Generally, pulsed lasers offer higher precision, but are less energy efficient and more expensive. The advantages/disadvantages of each laser type should be taken into consideration when selecting a modality to use in combination with MWNPs for image-guided PTT.

Beyond PA imaging, MRI and FL imaging, other techniques that have been used in combination with MWNPs for image-guided PTT include X-ray computed tomography (CT) imaging, surface enhance Raman scattering (SERS) imaging

and long-persistent luminescence imaging. The following subsections discuss the types of MWNPs that have been combined with each distinct modality for image-guided PTT.

2.1. MWNPs for dual PTT and PA imaging

PA imaging is a real-time imaging modality that combines the high contrast of optical imaging with the fine special resolution of ultrasound imaging. In PA imaging, short pulses of non-ionizing light are used to excite exogenous contrast agents embedded within tissue resulting in a temperature increase that produces pressure waves (i.e., thermoelastic expansions) detectable by an ultrasound transducer at the tissue surface [49]. Several small-molecule NIR dves like ICG. IR780 and IR1048 have been loaded inside MWNPs of various compositions for dual PTT and PA imaging [8,9,12,14]. Alternatively, MWNPs have been produced from materials with inherently high photothermal conversion efficiency such as semiconducting polymers, pigmented materials and gold [15,17,23,24,26,29]. While the NIR absorbance of gold-based NPs can be orders of magnitude larger than that of NIR dyes, allowing for greater contrast enhancement and heat production, the non-degradable nature of gold-based NPs raises concern of eventual metal-related cytotoxicity (though clinical trials indicate silica core/gold shell nanoshells have an excellent safety profile in humans) [6,7]. For this reason, much research into dual PTT/PA imaging has focused on MWNPs comprised of biocompatible and biodegradable materials, as discussed below.

2.1.1. NIR Dye-Loaded NPs for PTT/PA imaging

Several NIR dyes have been loaded in MWNPs to enable dual PTT and PA imaging, but the most common is ICG, which can support not only PTT and PA imaging, but also FL imaging. In one study, ICG-loaded PLGA NPs were coated with MCF-7 human breast cancer cell membranes that were modified with PEG so that they could engage the targeting ability of the cancer cell membranes along and the passivating properties of PEG (Figure 1A) [8]. When administered IV to nude mice bearing subcutaneous MCF-7 tumors, the ICGloaded cancer cell membrane-wrapped NPs (ICNPs) exhibited 3.1-fold and 4.75-fold greater tumor accumulation than unwrapped ICG-loaded NPs (INPs) and free ICG, respectively. Accordingly, the ICNPs provided higher contrast and better resolution than the other systems when PA and FL imaging of the tumors was performed (Figure 1B). Moreover, when the tumors were irradiated with an 808 nm laser (1 W/cm², 5 min) 24 h after IV injections, those that received ICNPs reached 55.3 °C, compared to only 48.2 °C for INPs (Figure 1C). The ICNP-mediated PTT induced complete tumor remission without relapse (Figure 1D), corresponding to 100% survival, compared to only 40% survival for INP-mediated PTT. These improved effects suggest that the dual tumor targeting and passivating provided by the PEG-modified cancer cell membrane coating was advantageous, though additional controls could have been included to demonstrate the benefit of PEG modified versus unmodified membranes.

By co-encapsulating drugs in NPs along with ICG, it is possible to achieve dual PTT and PA imaging along with chemotherapy. For example, Long et al. co-loaded ICG and doxorubicin (DOX) inside PEG-modified tungsten disulfide nanosheets that were further wrapped with folic acid (FA)modified RBC membranes [9]. In this system, the RBC membrane components enhance circulation while the FA modification enables targeting of cervical cancer cells that overexpress FA receptors. Compared to unwrapped nanosheets (PEG-modified tungsten disulfide (WS2) nanosheets carrying ICG and DOX (WID)) or RBC membrane-wrapped nanosheets lacking the FA modification (WID@M), the FA-modified RBC membrane-wrapped nanosheets (WID@M-FA) exhibited greater accumulation in subcutaneous HeLa tumors in nude mice 24 h after IV injection. Congruently, WID@M-FA NPs achieved the highest PA signal, which was 3.3-fold greater than that of the background, enabling ultra-sensitive and high-resolution imaging of the tumor morphology. When irradiated with 808 nm light (1 W/cm², 5 min), tumors of mice that received WID@M-FA NPs reached 54.9 °C, compared to 52.3 °C for WID@M NPs. After eight treatment cycles of NP injections and laser irradiation, the tumor inhibition rate achieved by WID@M-FA NPs was 95.4%, compared to 90.5% with WID@M NPs. The minimal difference in tumor inhibition between WID@M-FA NPs and WID@M NPs may be attributed to the repeated injection and irradiation cycles that magnified NP accumulation at the tumor site and hence minimized the benefit of the FA targeting. In future work, it would be interesting to compare tumor response after fewer rounds of treatment, which may better reveal the benefit, if any, of the FA modification.

Beyond ICG, other NIR dyes that have been loaded in MWNPs for dual PTT and PA imaging include IR780 and IR1048, the latter of which offers the benefit of NIR-II excitation [12,14]. In one example, RBC membrane-wrapped triblock copolymer NPs co-loaded with IR780 and the chemotherapy drug docetaxel (DTX) were evaluated for image-guided photo-chemotherapy of breast cancer in mice bearing subcutaneous MCF-7 tumors [12]. These NPs yielded greater PA signal and more effective tumor inhibition that unwrapped NPs loaded with IR780 and DTX, both in the absence and presence of 808 nm laser irradiation (i.e., chemo only or chemo + PTT), further confirming that RBC membrane coatings are beneficial when designing NPs for image-guided PTT. In an alternative approach that exploits the NIR-II window, liposomes were loaded with IR1048 and wrapped with platelet membranes to form BLIPO-1048, which exhibited impressive results in multiple tumor models, including xenografts of pancreatic cancer, breast cancer and glioma [14]. In particular, when administered to mice with orthotopic glioma xenografts, the BLIPO-1048 NPs achieved a PA imaging depth of 2.6 mm, with maximum contrast observed 12 h post-IV administration. The BLIPO-1048 NPs outperformed bare LIPO-1048 NPs, likely because P-selectin on the platelet membrane surface enabled targeting of CD44 receptors on the glioma cells. Upon 1064 nm laser irradiation (1 W/cm², 5 min), the BLIPO-1048 NPs increased tumor temperature to 45.3 °C, inhibited tumor growth rate by 85.2% (compared to only 57.9% for bare LIPO-1048 NP + laser) and extended

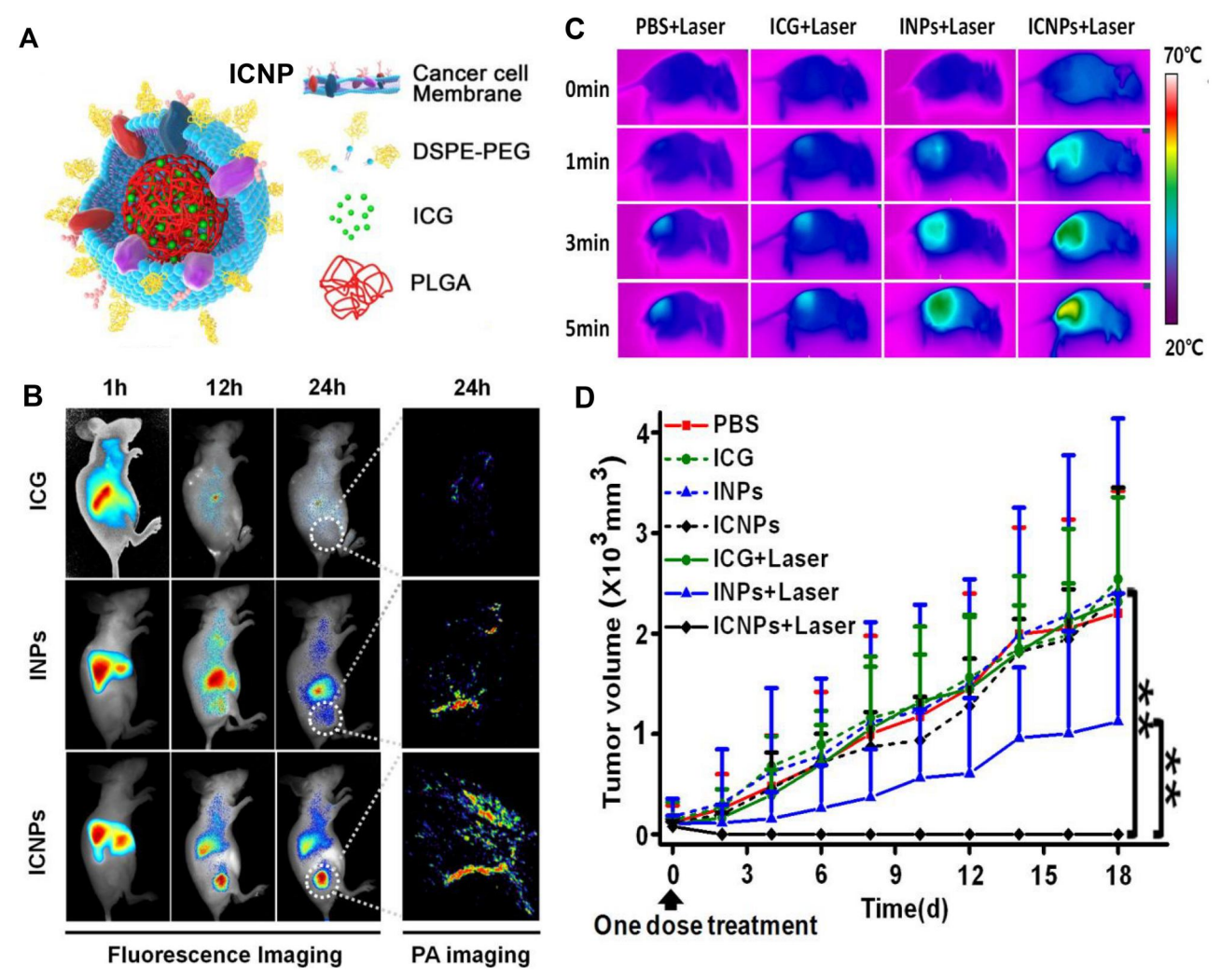


Figure 1. Representative MWNP used for PTT, PA imaging and FL imaging. (A) Scheme of ICNP. (B) FL and PA images of MCF-7 breast cancer tumors in mice following IV injection with either ICG, INPs or ICNPs. (C) Thermal images of MCF-7 tumor-bearing mice exposed to an 808 nm laser for 5 min (1 W/cm^2) after IV injection of PBS, ICG, INPs or ICNPs. (D) Tumor growth curves of different groups after treatments (n = 5). Reprinted (adapted) with permission from Chen et al. [8,p.10049]. Copyright 2016 American Chemical Society.

median survival time from 20 to 42 days. Overall, this example and the ones above warrant further investigation of NIR dye-loaded MWNPs for PA image-guided PTT of cancer.

2.1.2. Semiconducting materials for combined PA imaging and PTT

Semiconducting polymer nanoparticles (SPNs) are another promising platform that has been explored for image-guided PTT of cancer, as their excellent photonic properties allow them to support PA imaging, FL imaging and PTT. One elegant example is poly-(cyclopentadithiophene-alt-benzothiadiazole) (PCPDTBT) NPs, which were wrapped with activated fibroblast membranes to form AF-SPNs capable of multimodal cancer phototheranostics [15]. The use of activated fibroblast membranes is a unique and sophisticated approach to target homologous cancer-associated fibroblasts in the tumor microenvironment, which surround the tumor and produce extracellular matrix components and thus act as a physical barrier that impedes NP delivery deep within tumors [50]. To test the tumor-targeting ability of AF-SPNs

in vivo, nude mice bearing 4T1 xenografts were IV injected with either AF-SPNs, unwrapped SPNs (uSPNs) or 4T1 murine breast cancer cell membrane-wrapped SPNs (CC-SPNs). At 48 h post IV injection, the maximal PA intensity enhancement (ΔPA) in the tumors of AF-SPN treated mice was 1.8- and 1.5-fold higher than that for uSPN and CC-SPN treated mice, respectively. These results were consistent with FL images in which the tumor FL intensity of AF-SPN treated mice was 1.5- and 1.3-fold higher than that of uSPN and CC-SPN injected mice, respectively. After tumors were exposed to 808 nm light (0.3 W/cm², 5 min), the maximal tumor temperature was 50 °C for AF-SPN injected mice, which was 4.0 and 6.0 °C higher than that for CC-SPN and uSPN injected mice, respectively. Congruently, tumor volumes decreased to the greatest extent in mice that received irradiation plus AF-SPNs. Overall, this study confirmed that targeting activated fibroblasts with MWNPs is a promising approach to enhance cancer imaging and PTT. Other work has shown that SPNs based on a different material that are wrapped with RBC membranes can potently image and treat 4T1 tumors in mice [16]. Future studies that use the same core but different

membrane coatings (activated fibroblasts, cancer cells, RBCs) would be extremely valuable in guiding the design of MWNPs for dual cancer imaging and PTT.

Beyond single membrane coatings, hybrid membrane coatings have also been explored in combination with semiconducting materials for dual PA imaging and PTT of cancer. For instance, DOX-loaded hollow copper sulfide NPs have been coated with hybrid RBC and B16-F10 melanoma cell membranes to produce DCuS@[RBC-B16] NPs for combination imaging/PTT/chemotherapy of melanoma (Figure 2A) [25]. Unlike gold-based nanoprobes whose optical absorbance varies with the surface plasmon resonance, the optical properties and NIR absorption of copper sulfide NPs is based on energy band-band transitions of Cu²⁺ ions [9]. When administered IV to nude mice bearing subcutaneous B16-F10 xenografts, CuS@[RBC-B16] NPs (without DOX loaded) achieved a strong localized PA signal in the tumor 4h postinjection (Figure 2B). Additionally, the CuS@[RBC-B16] NPs had a similar blood retention time to NPs that had only an RBC membrane coating, which was greater than the retention of NPs with B16-F10 coatings or no coating (Figure 2C). Owing to the combined long-circulation and homotypic targeting properties of the hybrid membrane coating, the CuS@[RBC-B16] NPs exhibited the greatest tumor delivery (Figure 2D). Accordingly, when tumors were irradiated with 1064 nm light (1 W/cm², 5 min) both CuS@[RBC-B16] NPs and DCuS@[RBC-B16] NPs vielded impressive tumor growth inhibition (Figure 2E). Collectively, these data indicate that hybrid membrane coating is advantageous when designing theranostic MWNPs.

2.1.3. Pigmented materials for combined PA imaging and PTT

Pigmented materials can also support dual PA imaging and PTT. Examples include melanin, a natural organic polymer derived from tyrosine which has semiconducting properties, and Prussian blue, an inorganic dark blue pigment derived from oxidation of ferrous ferrocyanide salts. In one study, melanin was extracted from cuttlefish ink sacs to create NPs that were then wrapped with RBC membranes for enhanced PTT and PA imaging [23]. The Melanin@RBC NPs and bare melanin NPs were IV injected into Balb/c nude mice bearing A549 subcutaneous lung tumors and at 4h post-injection the Melanin@RBC NPs exhibited a 1.35-fold enrichment of PA tumor signal intensity compared to unwrapped melanin NPs. By 24h, the PA signal in the tumor dropped significantly,

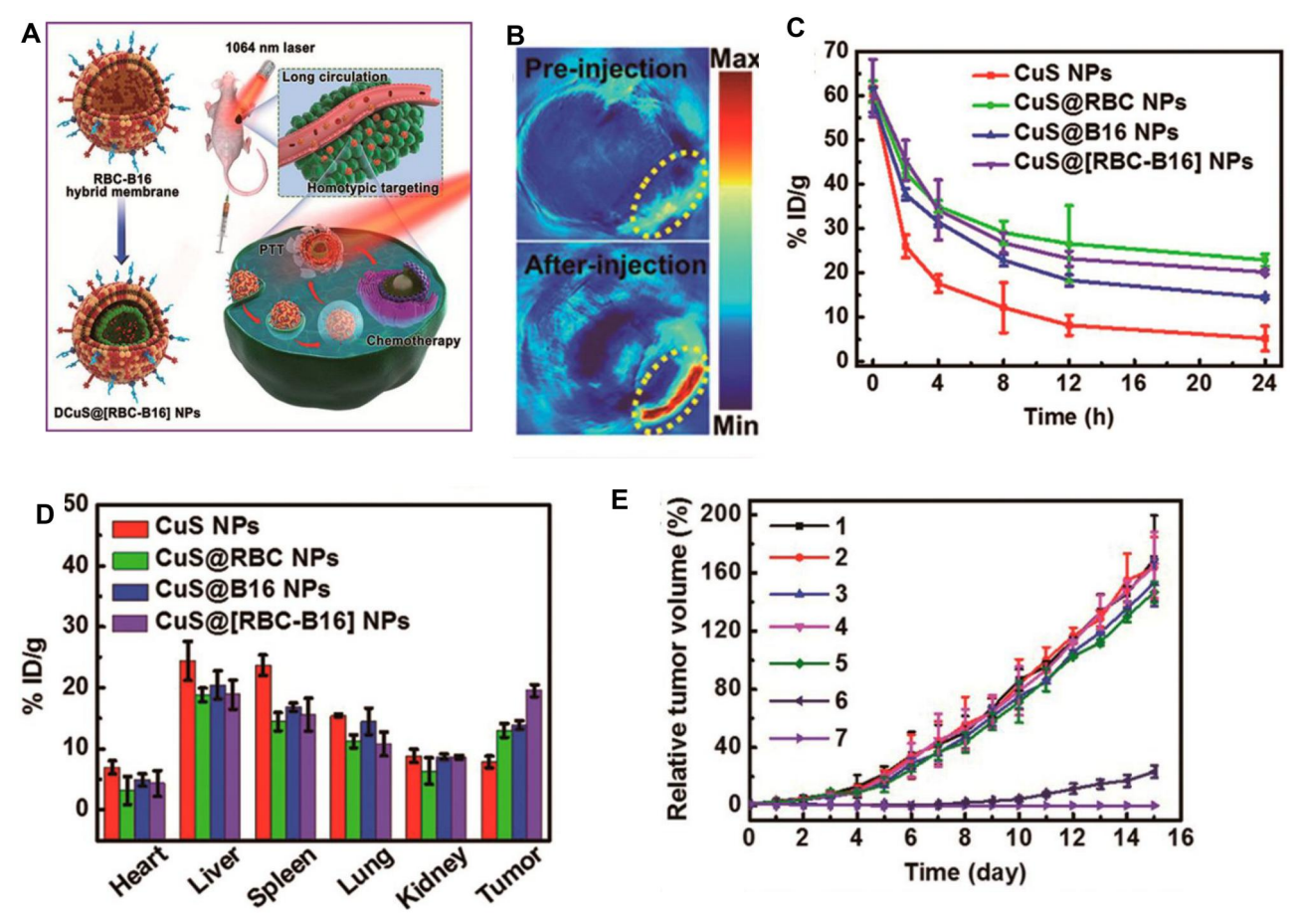


Figure 2. Representative example of membrane-wrapped semiconducting material for combined PTT and PA imaging. (A) Hybrid membrane-coated DOX-loaded hollow cupper sulfide NPs (DCuS@[RBC-B16] NPs) were explored for combination imaging/PTT/chemotherapy of melanoma. (B) CuS@[RBC-B16] NPs achieved a strong localized PA signal in tumors 4 h post IV injection. (C) Blood retention time of CuS NPs that were unwrapped or coated with RBC membranes, B16-F10 membranes or hybrid RBC-B16 membranes. (D) Biodistribution of unwrapped, RBC-wrapped or hybrid membrane-wrapped CuS NPs in tumor-bearing mice after IV injection. (E) Relative tumor volume of mice exposed to different treatments (1: NS, 2: CuS@[RBC-B16], 3: DOX, 4: NIR laser (1064 nm, 1 W/cm²), 5: DCuS@[RBC-B16], 6: CuS@[RBC-B16] with NIR laser, 7: DCuS@[RBC-B16] with NIR laser). Reprinted (adapted) with permission from Wang et al. [25,p.5241]. Copyright 2018 American Chemical Society.

which the authors attributed to potential degradation of the NPs by hydrogen peroxide (H_2O_2) produced by surrounding cancer cells. When tumors of NP-injected mice were irradiated with 808 nm light ($2\,\text{W/cm}^2$, $5\,\text{min}$) 4 h post-injection, the Melanin@RBC NPs had an approximately 100% antitumor rate, compared to bare melanin NPs that had $\sim 78\%$ tumor inhibition. When irradiated at a lower power density of 1 W/cm² for 10 min, the Melanin@RBCs still provided significant tumor inhibition that was much greater than that of unwrapped melanin NP controls.

In related work, melanin NPs have been coated with hybrid membranes derived from RBCs and MCF-7 human breast cancer cells to produce Melanin@RBC-M NPs for dual imaging/PTT [24]. Hybrid membranes were made with varying source membrane ratios and the ratio of 1:1 RBC:MCF-7 provided an optimal balance between the prolonged blood circulation of RBC membranes and the homotopic targeting of MCF-7 cell membranes. Further studies evaluated the sizedependent PA imaging, tumor accumulation and photothermal performance of Melanin@RBC-M NPs in nude mice bearing subcutaneous MCF-7 tumors by varying the melanin core size (64, 93, 124 and 148 nm). PA signal and tumor accumulation decreased as NP size increased and, regardless of core size, the PA signal plateaued 4h after IV injection. When tumors in the same animal model were irradiated with an 808 nm laser (1 W/cm², 10 min), Melanin@RBC-M NPs with a 124 nm core yielded the greatest tumor temperature increase (from 29.6 to 54.0 °C). PTT mediated by this hybrid membrane-wrapped formulation caused complete tumor elimination, while PTT mediated by RBC membrane-wrapped or unwrapped melanin NPs caused 92.3% or 30% tumor inhibition, respectively. These data, like those for the CuS NP system described above, again demonstrate hybrid membrane coatings are beneficial compared to single membrane coatings.

The other major pigmented material explored as a dual PA imaging/PTT agent is Prussian blue. Recent work demonstrated that membrane-wrapped Prussian blue NPs can enable mild-temperature PTT [26]. When tumor tissues are heated above 50 °C, it can trigger inflammation that facilitates undesirable immune escape and metastasis or induce nonspecific necrosis in surrounding healthy tissues. To avoid these complications, mild-temperature PTT that heats tumors to less than 45 °C has been explored. Wang et al. synthesized zinc-glutamate-modified Prussian blue NPs that were loaded with triphenylphosphine (TPP)-conjugated lonidamine and then wrapped with HepG2 hepatocellular carcinoma cancer cell membranes. Lonidamine is an anticancer drug that reduces tumor cells' energy production by inhibiting glycolysis and mitochondrial respiration, so it was conjugated to the mitochondria-targeting group TPP to enhance its effect. Nude mice bearing subcutaneous HepG2 tumors were IV injected with either unwrapped or membrane-wrapped NPs, which achieved relative PA signal in tumors of 2.6 and 4.4 at 12 h post-injection. When tumors were irradiated with an 808 nm laser (1 W/cm², 5 min), the tumor temperature increased to 44.9 ± 1.7 °C for the membrane-wrapped NPtreated mice, which caused a tumor inhibition rate of 89.2%

after 16 days of monitoring, confirming the therapeutic potential of mild-temperature PTT. Overall, these NPs provided targeted drug delivery, effective mild-temperature PTT and enhanced PA imaging. A noted improvement that could be made to this nanoformulation or similar ones would be to develop a simpler and more facile design for easier clinical translation.

2.2. MWNPs for combination MRI and PTT

2.2.1. Membrane-wrapped iron oxide NPs as phototheranostics

Compared to optical imaging techniques, MRI offers the advantage of deep tissue imaging with high resolution and contrast, with the tradeoff of reduced imaging speed. Iron oxide (Fe₃O₄) NPs are the most widely used material for dual PTT/MRI, because they are excellent T2-weighted MRI contrast agents that also offer good biocompatibility and high stability in physiological environments [22]. Several groups have wrapped Fe₃O₄ magnetic nanoclusters (MNCs) with cellderived membranes for image-guided PTT [19–22,51]. Examples include MNCs wrapped with RBC membranes for MRI-enhanced PTT of breast cancer and cervical cancer [20-22], MNCs wrapped with myeloid-derived suppressor cell (MDSC) membranes for melanoma imaging/treatment [19], and iron oxide NPs wrapped with mesenchymal stem cell (MSC) membranes for prostate cancer imaging/treatment [51]. Across studies, membrane-wrapped formulations have provided greater tumor contrast and photothermal ablation than uncoated formulations. Additionally, MDSC membranewrapped MNCs have provided greater tumor targeting, MRI contrast and PTT than RBC-wrapped MNCs, likely because MDSCs expeditiously accumulate in tumors in response to cytokines and chemokines released from the inflammatory tumor microenvironment [19].

Of note, one study compared RBC membrane-wrapped Fe₃O₄ NPs produced by conventional mechanical extrusion (RBC-MN-Cs) to those prepared by microfluidic electroporation (RBC-MN-Es) [20]. After IV injection into Balb/c nude mice bearing MCF-7 xenografts, MR imaging showed RBC-MN-Es yielded superior darkening of tumor regions 24 h post-injection compared to RBC-MN-Cs and unwrapped MNs, indicating more tumor accumulation. RBC-MN-Es also exhibited lower enrichment in the spleen and liver after 48 h, demonstrating superior avoidance of MPS clearance organs. Finally, RBC-MN-Es provided more potent PTT upon 808 nm laser irradiation. Collectively, these results give evidence that microfluidic electroporation may provide more complete/ effective cell membrane coatings than conventional extrusion. Further study of microfluidic electroporation is important for the future translation of theranostic MWNPs into industrially manufactured products.

Beyond modifying the membrane type or coating technique to enhance tumor delivery, MR contrast and PTT efficacy, another tactic to enhance dual imaging/PTT is to use materials that support NIR-II excitation or combination therapy. For example, Lin et al. created core-shell or rattle-type Fe_3O_4 @CuS NPs wrapped in RBC membranes that could be

guided to tumors by external magnetic fields, which allowed for enhanced MRI and PTT within the NIR-II window that allows deeper tissue penetration and increased maximum permissible light exposure [21]. In a different approach, Mu et al. modified hydrophobic iron oxide NPs with a polydopamine coating that facilitated adsorption of small interfering ribonucleic acid (siRNA) for gene regulation, and these NPs were coated with MSC membranes for imaged-guided PTT and siRNA delivery to human DU145 prostate cancer xenografts in Balb/c mice [51]. After the NPs were IV injected, there was obvious tumor darkening in T2-weighted MR images taken 24h post-injection compared to unwrapped control NPs, and ICP-AES at 48 h confirmed greater tumor accumulation of the MSC MWNPs. The MWNPs designed to provide both PTT and siRNA-mediated silencing of an overexpressed proto-oncogene reduced tumor volume by 60% when combined with 808 nm light (0.6 W/cm², 6 min) compared to 40% for non-targeting NPs combined with irradiation. It was shown that the MSC coating benefited MR image contrast, as well as increased the therapeutic effects of the delivered siRNA and PTT [51]. Future work should continue to explore new approaches to enhance the success of MWNPs for combination MR imaging and therapy. In particular, researchers should develop MWNPs as positive contrast agents for T1-weighted MRI, which could be advantageous over the use of MWNPs as negative contrast agents for T2weighted MRI.

2.2.2. Triple-modality MWNPs for MR, PA and FL imaging

Since different imaging techniques offer distinct benefits and drawbacks, it is desirable to develop MWNPs that support multimodal imaging and thereby improve the precision and sensitivity of imaging or provide more information about the NP location or tumor properties. In one exciting example, A549 lung cancer cell membrane camouflaged NPs were designed for triple-modality MRI, FLI and PAI for accurate tumor diagnostics and effective antitumor treatment [47]. This system consisted of PLGA NPs loaded with ICG along with perfluoro-15-crown-5-ether (PFCE), an excellent ¹⁹F MRI agent. For in vivo evaluation, the A549 membrane-wrapped PFCE- and ICG-loaded NPs (AM-PP@ICGNPs) or unwrapped controls were IV injected into nude mice bearing A549 tumor xenografts at an ICG concentration of 200 μg/mL. A strong FL intensity was achieved in tumors of AM-PP@ICGNPs treated mice at 24 h and steadily persisted through 48 h, with intensity 3.6-fold higher than the waning signal achieved by bare NPs at 48 h. At 24 h, the PA signal intensity of AM-PP@ICGNPs inside tumors was 1.4-fold higher than that of unwrapped controls. Moreover, there was a 2.37 intratumoral ¹⁹F MRI intensity for AM-PP@ICGNPs compared to only 0.84 for unwrapped controls. To assess PTT efficacy in vivo, mice bearing A549 tumors received wrapped NPs or controls IV and were subsequently irradiated with a 765 nm laser at 400 mW/cm² for 15 min. At the end of three treatperiods and 18 days of monitoring, PP@ICGNPs + laser reduced tumor volumes by 86% where other treatment groups only experienced progressive tumor growth. In sum, AM-PP@ICGNPs could inhibit tumor growth

while also supporting multimodal tumor imaging [47]. Such multimodality systems have great promise for future clinical use as anticancer treatments while ensuring high precision imaging of tumor regions throughout the treatment process. However, multimodal imaging may require increased time and cost, so researchers and clinicians must carefully consider the cost/benefit ratio when making decisions on the best modality/modalities to use for a particular indication.

2.3. Membrane-wrapped NPs for dual PTT and FL imaging

To facilitate FL imaging and PTT of tumors, NIR dyes like ICG are typically loaded in polymeric NPs [10] or liposomal NPs [11], which can be wrapped with cell membranes to enhance tumor delivery. While this approach has been widely explored, this section focuses on formulations that have been used to image and treat glioblastoma.

Glioblastoma is particularly challenging to treat because IV-administered therapies must bypass tight junctions in the blood-brain barrier (BBB) and blood-tumor barrier (BTB) that block about 98% of small-molecule or macromolecule drugs and contrast agents from entering the brain [10]. To overcome this barrier, one group synthesized copolymer NPs loaded with ICG, which were wrapped with membranes derived from various types of metastatic cancer cells to enable them to traverse the BBB and perform FL imaging and PTT. The membrane sources evaluated included metastatic mouse melanoma cells (B16-F10), metastatic murine mammary carcinoma cells (4T1) and normal fibroblast cells (COS-7). The ability of these membrane-coated NPs to cross the BBB and facilitate FL imaging of tumors was evaluated in animal models with different degrees of BBB disruption at different stages of disease development. In healthy mice with an intact BBB, animals treated with B16-F10 and 4T1 MWNPs had 15- and 14-times higher FL intensities in the brain 8h after IV injections than bare NP-treated mice, showing that coating NPs with metastatic cancer cell membranes is promising for early-stage diagnosis of brain tumors when the BBB is mostly intact. Subsequent studies examined delivery to orthotopic U87MG-Luc glioblastoma tumors either 7 days or 14 days post tumor cell inoculation, where the later-stage tumors are larger and exhibit greater levels of BBB disruption. In mice with 'early-stage disease' (7 days post-cell inoculation), the FL signal in tumors 8h post IV injection was approximately 11-fold higher in mice that received MWNPs compared to bare NPs and in the 'latestage tumor model' (14 days post-cell inoculation) the difference was 5 times. The reduced difference between wrapped and unwrapped NPs in the later-stage disease model may be attributed to the greater level of BBB disruption allowing more unwrapped NPs to passively accumulate in tumors. Importantly, the improved BBB penetration and tumor delivery achieved by the MWNPs also allowed them to increase PTT efficacy. In a therapeutic study, B16- or COS7-MWNPs were IV administered to mice bearing orthotopic gliomas 7 days post cell inoculation. Eight hours after IV injections, glioma sites were irradiated with an 808 nm laser (1 W/cm²,

5 min). Tumors of B16-MWNP + laser treated mice heated to 48 °C while those of COS7-MWNP + laser treated mice only rose to 39.8 °C, which is below the minimum temperature needed to cause irreversible tissue damage. Collectively, these results confirmed NPs coated with metastatic cancer cell membranes can successfully traverse the BBB in healthy and cancer conditions to act as an effective FL imaging tool and PTT agent.

Similar results were obtained in a study where liposomes loaded with ICG were wrapped with C6 rat glioma cell membranes [11]. The wrapped and unwrapped liposomes were tested in later-stage (14 days post C6 cell inoculation) and earlier-stage (7 days post C6 cell inoculation) orthotopic glioma mouse models to assess efficiency at crossing the BBB for FL imaging and PTT. As expected, the wrapped liposomes outperformed their unwrapped counterpart as both a tumor FL imaging agent and a PTT mediator in both stages of disease. Beyond ICG, the NIR dye IR792 has also been loaded in polymer-based NPs that were wrapped with macrophage membranes to provide successful FL imaging and PTT of glioblastoma [13]. The advantage of macrophages as a coating is that they contain proteins such as integrin $\alpha 4$ and macrophage-1 antigen that are responsible for penetrating the BBB and targeting glioblastoma. When tested in nude mice bearing orthotopic glioblastoma, these NPs reached an apex of FL intensity 24h after IV injections. Moreover, they clearly delineated tumors with a high SNR of 4.16 compared to 1.03 SNR for free IR792 and 1.05 SNR for unwrapped NPs (Figure 3A). When administered to healthy nude mice, the MWNPs exhibited FL in the brain at 6 h, indicating they may be able to cross the BBB even in healthy brains with normal vasculature and tight junctions. As anticipated, when tumorbearing mice were treated with the IR792-loaded MWNPs and laser irradiation, they effectively suppressed tumor growth and increased median survival time to 22 days compared to 16 days for unwrapped NPs plus laser or 14 days for saline control (Figure 3B,C). These results, coupled with those for ICG platforms above, demonstrate the potential of NIR dye-loaded MWNPs to enhance imaging and therapy of early-stage or late-stage glioblastoma. Moving forward, it will be important for researchers to determine what components/features of the membranes in MWNPs (e.g., specific proteins, phospholipids, carbohydrates) are enabling their improved passage across the BBB. As the BBB is one of the most challenging vascular barriers to penetrate, understanding the structure-function relationship of these materials might be extremely informative to fields of (nano)medicine focused on enabling treatment of cancers and other diseases impacting the brain.

2.4. MWNPs for image-guided PTT using other imaging techniques

Beyond PA, MR and FL imaging, many other imaging modalities can be combined with phototherapeutic NPs for imageguided cancer therapy, including X-ray CT, surface-enhanced Raman scattering (SERS) and long-persistent luminescence imaging. These alternative techniques are discussed below.

CT is an attractive imaging modality because it provides high resolution, no depth limitation and 3D reconstruction options. While a wide variety of NPs are being developed as CT contrast agents (including those based on gold, iron oxide and dyes like ICG), bismuth (Bi)-based NPs are particularly promising owing to their high X-ray attenuation coefficient, which gives them superior imaging capabilities [52,53]. Zhao et al. developed quercetin (QE)-loaded hollow bismuth selenide (Bi₂Se₃) NPs camouflaged with macrophage membranes (M@BS-QE NPs) for multimodal imaging and therapy of breast cancer [28]. QE was added to the NP cores to inhibit heat shock protein 70 (HSP70) and thereby reduce tumor cell resistance to PTT. QE was also used because it can limit tumor cell proliferation by inhibiting the expression of protein kinase B (Akt) and active Caspase-3 via downregulation of the p-Akt/MMP-9 signal pathway. Macrophages were selected as the membrane exterior to exploit the $\alpha 4$ integrin/vascular cell adhesion molecule-1 (VCAM-1) interaction between macrophages and cancer cells and the C-C chemokine ligand 2 (CCL2)/CCR2 chemokine axis, which should increase NP targeting of primary tumors, their stromata and pulmonary metastases. The goal was to use this platform for targeted hyperthermia and triggered QE release. For antitumor phototherapy studies, Balb/c mice bearing subcutaneous 4T1 breast cancer tumors were IV injected with M@BS-QE NPs then tumors were subjected to 808 nm laser irradiation (2 W/cm 2 , 5 min). M@BS-QE NPs + laser treated mice experienced sharp reduction in tumor volumes and the greatest amount of cell apoptosis within tumors, while maintaining body weight indicative of low systemic toxicity. $M@BS-QE\ NPs+laser\ treated\ mice\ also\ exhibited\ the$ greatest down-regulation of MMP9 expression, suggesting successful QE release. To analyze CT imaging capabilities, 4T1 subcutaneous tumor-bearing mice were intratumorally injected with M@BS or lohexol, a commercial CT contrast agent. M@BS had a much higher CT value at the tumor site (~295 HU) compared to those treated with lohexol (\sim 183 HU), showing its success as a CT contrast agent. Future work should examine CT contrast after IV delivery. To assess the antimetastatic potential of M@BS-QE NPs, a breast cancer lung metastasis model was established in Balb/c mice by injecting 4T1 cells into the tail veins. After IV injection of various treatments without irradiation, the percentage of mice with metastatic nodules was 100% for phosphate buffered saline (PBS), 75% for free QE, 66% for BS-QE NPs and 17% for M@BS-QE NPs. The success of M@BS-QE NPs to prevent lung metastasis was attributed to the active cancer cell targeting ability of the macrophage membranes. Overall, the biomimetic Bi-based NPs could successfully perform PTT, provide hyperthermia-triggered drug release, enhance CT imaging of tumors and limit lung metastasis. Future work should further explore the ability of these and other NPs to enhance CT contrast and treatment of primary tumors and metastases after IV (rather than intratumoral) injection.

Another less utilized but very promising technique is SERS imaging, which relies on the ability of NPs to enhance the Raman scattering of tethered molecules. In one study, gold nanodendrites (AuNDs) loaded with ICG were used for

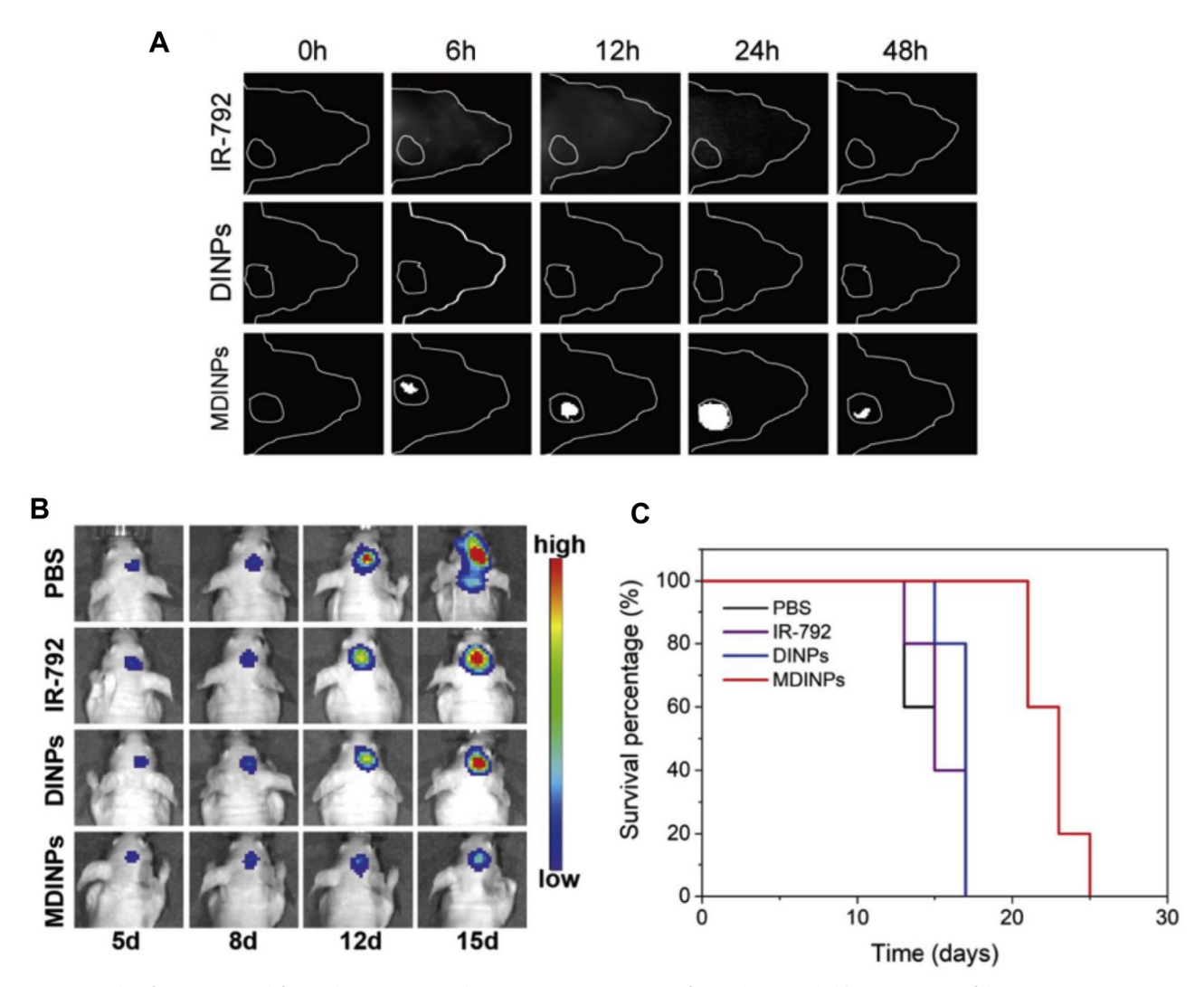


Figure 3. Example of a MWNP used for dual FL imaging and PTT. (A) NIR-II FL images of mice bearing glioblastoma tumors following IV injection with either IR792, DINPs (unwrapped NPs loaded with IR792) or MDINPs (macrophage membrane-wrapped NPs loaded with IR792). (B) Representative bioluminescence images of tumors after treatment with different agents combined with 808 nm irradiation. (C) Survival rates of mice in different groups after PTT (n = 5). Reprinted (adapted) with permission from Lai et al. [13,p.48]. Copyright 2019 American Chemical Society.

combination NIR-I activated photodynamic therapy (PDT), NIR-II activated PTT, PAI, FLI and SERS imaging [18]. The AuNDs were coated with RAW 264.7 macrophage membranes to enable targeted delivery to MDA-MB-231 human breast cancer cells via the active binding of macrophageexpressed $\alpha 4$ integrins to overexpressed VCAM-1 on MDA-MB-231s. The AuNDs were also conjugated with a mitochondria-targeting cationic compound, TPP, to help deliver the ICG specifically to mitochondria once inside target cells to increase PDT efficacy and enable SERS imaging. The complete formulation was termed AuND-TPP-ICGs@MCM. When IV injected into nude mice with subcutaneous MDA-MB-231 tumors, AuND-TPP-ICG@MCM successfully enabled FL imaging (Ex: 640 nm, Em: 720 nm), NIR-II PAI (Ex: 1200 nm via a visual sonic system) and SERS imaging (Ex: 785 nm diode laser). The NPs also successfully mediated PTT and PDT upon excitation with 1064 nm (1.0 W/cm², 10 min) and/or 808 nm (0.3 W/cm², 5 min) light. This unique system nicely demonstrates the ability to provide NIR-II PTT and NIR-I PDT along with FL, PA and SERS imaging in a single NP platform.

Finally, a relatively new field of biomedical imaging uses NIR persistent luminescence nanoparticles (PLNPs) to overcome the tissue autofluorescence that limits traditional FL imaging. Because PLNPs emit luminescence even after excitation has ceased, they can achieve a high SNR. One platform for dual persistent luminescence imaging and PTT was developed from Zn_{1,25}Ga_{1,5}Ge_{0,25}O₄:Cr³⁺,Yb³⁺,Er³⁺ (ZGGO) coated with mesoporous silica, which was further loaded with IR825 and the chemotherapeutic drug irinotecan (Ir) [27]. The NPs were coated with hybrid membranes made from a 1:1 ratio of CT26 murine colorectal carcinoma cell membranes and RAW 264.7 murine macrophage membranes, resulting in the final platform termed IR825/Ir ZGGO@ SiO₂@CMM. In vivo studies in Balb/c mice bearing subcutaneous CT26 tumors showed that the hybrid membrane-wrapped NPs provided greater contrast enhancement, PTT effects and chemotherapy than NPs coated with only CT26 or only macrophage membranes, further supporting the concept that hybrid membrane coatings are advantageous to membrane coatings derived from a single cell type. Future research into PLNPs



may further demonstrate the benefits of these systems over traditional FL imaging contrast agents for image-guided cancer therapy.

Overall, as new imaging techniques are developed and combined with phototherapeutic NPs, the imaging and treatment of tumors is expected to continually improve. Ultimately, these advances will benefit patients by ensuring complete tumor elimination without fear of relapse.

3. Conclusions: perspective on the path forward for MWNPs for image-guided PTT

Cell membrane-wrapped theranostic NPs show great promise to enhance the imaging and treatment of solid-tumor cancers in murine models. Table 3 summarizes the different systems presented in this review. As highlighted here, MWNPs consistently exhibit greater accumulation in tumors than their PEGylated or unwrapped counterparts, which allows them to provide better tumor contrast and heat tumors more effectively when activated by laser light in vivo. Importantly, wrapping theranostic NPs with cell membranes does not alter their optical properties or heating profiles and endows them with unique biointerfacing capabilities that are inherited from the source cells. These capabilities include immune evasion that prolongs the NPs' systemic circulation and thereby improves their passive tumor accumulation. Some membranes (such as those derived from cancer cells, macrophages, MDSCs and others) provide natural tumor-targeting abilities owing to specific cell adhesion molecules present on the membrane surface. Alternatively, targeting can be achieved by engineering non-targeting membranes such as those derived from RBCs to express targeting moieties. While MWNPs for dual imaging/PTT have shown tremendous promise in pre-clinical studies, more research is required for them to realize their full potential.

Some challenges that might limit the clinical translation of phototheranostic MWNPs to patient care include (i) the shallow penetration depth of NIR light in tissues, which makes it ineffective in imaging and eradicating deep tumors when applied externally, (ii) the heterogeneity and potential toxicity of some theranostic NPs owing to the materials incorporated and (iii) tumor thermal resistance. The issue of limited penetration depth could be overcome by designing theranostic NPs that absorb light in the NIR-II window rather than the NIR-I window, which has already been demonstrated as feasible [13]. Alternatively, fiber optic probes could be inserted into tumors to irradiate them from within, which is the approach that has been used in human clinical trials [5,6]. Regarding potential toxicity, although many of the reported systems have proven short-term biocompatibility in animal studies, their long-term safety needs to be addressed since a large amount of administered MWNPs accumulate in healthy tissues like liver and spleen [54]. The excellent safety profile of PEGylated nanoshells in humans is encouraging [7], but whether these or other NPs remain biocompatible when coated with cell-derived membranes remains to be elucidated. Another potential challenge to clinical translation of MWNPs is their inherently high heterogeneity owing to the

complexity of the cellular membrane components included in the design, which may limit manufacturing scale-up. The processes to collect large amounts of cell membranes and produce clinical doses of MWNPs with batch-to-batch consistency will need to be refined for this technology to become a clinical reality [43]. Finally, tumor thermal resistance is an issue that needs to be addressed as excessively heated cells can increase their expression of HSPs that prevent apoptosis, reducing the efficacy of PTT [55]. Mild-temperature PTT has been explored to address this issue, with promising results [26,56]. Some studies have shown that mild-temperature PTT can sensitize cancer cells to other therapies, and these synergistic effects allow for lower doses of each agent to be administered [57,58]. While each of these challenges individually is addressable, more research is needed to develop a system that can address all these limitations simultaneously.

Other areas of research that need to be addressed to advance the field of MWNPs for cancer imaging, PTT and other applications include understanding the fate and membrane integrity of IV-administered NPs after distribution. Although these particles exhibit high stability in serum conditions in vitro and extended circulation in vivo in mice, it is still unknown how the high shear stress and serum proteins in blood vessels might alter the structure/composition of the membrane layer surrounding MWNPs. Another underresearched area is how the tumor microenvironment affects the success of membrane-wrapped theranostic NPs. Most research in solid-tumor cancer PTT focuses on thermally ablating cancer cells, but the tumor microenvironment has numerous cell types that play a huge role in disease progression [59]. In one clever approach, NPs were wrapped with activated fibroblast membranes to target cancer-associated fibroblasts, with promising results [15]. Future research should further explore the ability to more completely target both cancer cells and stromal cells in the tumor microenvironment to maximize contrast enhancement and therapeutic efficacy.

As the field matures, it will be important to define the characteristics of phototheranostic MWNPs that maximize tumor delivery and efficacy. While prior research suggests NPs with diameter of 30–200 nm and neutral or negative zeta potential exhibit the greatest tumor delivery [60], more research is needed to define structure-function relationships for MWNPs specifically. We postulate that different membrane coatings will be required to maximize targeting of tumors in distinct locations (e.g., brain versus breast versus bone) since specific membrane-embedded proteins mediate the targeting capabilities of MWNPs, but this should be confirmed experimentally and through meta-analyses of literature. We also believe it will be important for membrane coatings to be complete (i.e., fully surround the NP) and stable in biological conditions to maximize tumor delivery. Whether the wrapping technique (extrusion, microfluidic mixing or sonication) influences the coating completeness and stability needs to be determined. Researchers will also need to consider the source of membranes for clinical applications. An ideal scenario would be to make personalized MWNPs

Table 3. Summary of studies that have developed MWNPs for image-guided PTT.

NP components	Membrane source(s)	Laser parameters for <i>in vivo</i> PTT	lmaging mode(s)	Tumor model	Citation
PLGA loaded with ICG	MCF-7 breast cancer modified with PEG	808 nm 1 W/cm ² 5 min	FL, PA	MCF-7 breast cancer	Chen et al. [8,p.10049]
PEG-modified tungsten disulfide nanosheets loaded with DOX and ICG	RBC modified with FA	808 nm 1 W/cm² 5 min	PA	HeLa cervical cancer	Long et al. [9,p.5088]
Poly(caprolactone) (PCL)–PEG–PCL triblock copolymer loaded with IR780 and DTX	RBC	9.8mm 808mm 1.5/cm² 5 min	FL, PA	MCF-7 breast cancer	Yang et al. [12,p.3208]
Semiconducting PCPDTBT	Activated fibroblast	9.8.mm 808.nm 0.3.W/cm ² 5.min	FL, PA	4T1 breast cancer	Li et al. [15,p.8520]
Narrow bandgap electron donor–acceptor semiconducting polymer Acceptor segment: thiophene-fused benzodifurandione-based oligo(p-phenylene vinylene) Donor segment: thieno[3,2-b]thiophen-2-yl)	RBC	808 nm 0.5 W/cm ² 10 min	PA	4T1 breast cancer	Zheng et al. [16]
Hollow copper sulfide loaded with DOX	Hybrid: B16-F10 melanoma and RBC	1064 nm 1 W/cm² 5 min	PA	B16-F10 melanoma	Wang et al. [25,p.5241]
Melanin	RBC	2 W/cm ² , 5 min or 1 W/cm ² , 10 min	PA	A549 lung cancer	Jiang et al. [23,p.29]
Melanin	Hybrid: MCF-7 breast cancer and RBC	808 nm 1 W/cm² 10 min	PA	MCF-7 breast cancer	Jiang et al. [24,p.292]
Prussian blue NPs modified with zinc glutamate and with TPP conjugated lonidamine	HepG2 liver cancer	808 nm 1 W/cm² 5 min	PA	HepG2 liver cancer	Wang et al. [26,p.37563]
Gold nanostars	RBC	785 m 2 W/cm ² 5 min	PA	HepG2 liver cancer	Huang et al. [17]
Liposome loaded with IR1048	Platelet	1 W/cm ² 5 min	PA	C6 glioma	Geng et al. [14,p.55624]
Fe ₃ O ₄	RBC	5 min 808 mm 5 W/cm ² 5 min	MRI	MCF-7 breast cancer	Ren et al. [22,p.13]
Fe ₃ O ₄	RBC	5 W/cm ² 5 W/cm ² 5 min	MRI	MCF-7 breast cancer	Rao et al. [20,p.3496]
Fe ₃ O ₄	MDSC	808 nm 5 W/cm ² 5 min	MRI	B16-F10 melanoma	Yu et al. [19]
$Fe_3O_4@Cu_23S$	RBC	1064 nm 0.8 W/cm ² 10 min	MRI	HeLa cervical cancer	Lin et al. [21,p.1202]
Fe_3O_4 coated with polydopamine and siRNA	MSC	808 nm 0.6 W/cm² 6 min	MRI	DU145 prostate cancer	Mu et al. [51,p.3895]
					(continued)

_	_
1.	٠,
(=	0
	٠,

Table 3. Continued.					
ND components	Membrana cource(c)	Laser parameters	lmaging mode(s)	Timor model	(itation
	Melliblaile 30alce(3)		(E)appli	ווסמפון ווסמפון	Citation
PLGA loaded with ICG and PFCE	A549 lung cancer	765 nm 400 mW/cm²	PA, MRI, FL	A549 lung cancer	Li et al. [47,p.57290]
		III CI			
PCL and pluronic copolymer F68 NP loaded with ICG	B16-F10 melanoma, 4T1 breast cancer or COS7 fibroblast	808 nm 1 W/cm²	F	U87 glioblastoma	Wang et al. [10]
		5 min			
Liposomes loaded with ICG	C6 glioma	808 nm 1 W/cm ²	7	C6 glioma	Jia et al. [11,p.386]
		5 min			
DSPE-PEG NPs loaded with IR792	Macrophages	808 nm	FL	U87 glioblastoma	Lai et al. [13,p.48]
		u.s w/cm 5 min			
Hollow Bi ₂ Se ₃ loaded with QE	Macrophage	808 nm	FL, CT	4T1 breast cancer	Zhao et al. [28,p.31124]
		2 W/cm² 5 min			
AuNDs loaded with ICG and functionalized with TPP	Macrophage	1064 nm,	FL, PA, SERS	MDA-MB-231 breast cancer	Sun et al. [18,p.10778]
		1 W/cm ² , 10 min and/or 808 nm, 0.3 W/cm ² , 5 min	imaging		
Black-titanium (TiO ₂) NPs functionalized with iridium	HeLa cervical cancer	1064 nm	PA, two-photon	HeLa cervical cancer	Shen et al. [29,p.120979]
complexes		1 W/cm² 10 min	imaging		
ZGGO coated with mesoporous silica and loaded	Hybrid: CT26 colorectal cancer	808 nm	Long persistent	CT26 colorectal cancer	Wang et al. [27,p.7105]
with IR825 and Ir	and KAW 264.7 macrophage	1 W/cm² E mis	luminescence imaging		
) IIIIII			

using membranes sourced from a patient's own cells (such as collecting cancer cell membranes from cells collected during a tumor biopsy), as this would minimize the potential for immune response. However, if this is not feasible, an alternative approach could be to source more abundant RBC or leukocyte membranes from donors with blood-type compatibility and modify them with targeting moieties if desired [43]. Such membrane-sourcing and scale-up considerations will be critical to the successful clinical implementation of MWNPs for dual tumor imaging and PTT.

To conclude, membrane-wrapped theranostic NPs have great potential for image-guided PTT of solid-tumor cancers, but challenges to their clinical translation exist. Once these challenges are addressed, MWNPs for dual cancer imaging and PTT are likely to transform patient care.

Disclosure statement

The authors report there are no competing interests to declare.

Funding

This work was supported by the National Science Foundation (NSF) under grant number DMR1752009. Funding was also provided by the National Institutes of Health (NIH) under award number R01CA211925 and R35GM149292. GK acknowledges support from the graduate traineeship program NRT-HDR: Computing and Data Science Training for Materials Innovation, Discovery, Analytics (MIDAS) funded by NSF grant number 2125703.

ORCID

Sara B. Aboeleneen (i) http://orcid.org/0000-0003-1068-4349 Mackenzie A. Scully (i) http://orcid.org/0000-0001-6443-4287 George C. Kramarenko (i) http://orcid.org/0000-0002-6990-5620 Emily S. Day (ii) http://orcid.org/0000-0002-8707-826X

Data availability statement

Data sharing is not applicable to this article as no new data were created or analyzed in this study.

References

- [1] Siegel RL, Miller KD, Wagle NS, et al. Cancer statistics, 2023. CA Cancer J Clin. 2023;73(1):17–48. doi: 10.3322/caac.21763.
- [2] Alieva M, van Rheenen J, Broekman MLD. Potential impact of invasive surgical procedures on primary tumor growth and metastasis. Clin Exp Metastasis. 2018;35(4):319–331. doi: 10.1007/ s10585-018-9896-8.
- [3] Arruebo M, Vilaboa N, Sáez-Gutierrez B, et al. Assessment of the evolution of cancer treatment therapies. Cancers. 2011;3(3): 3279–3330. doi: 10.3390/cancers3033279.
- [4] Riley RS, Day ES. Gold nanoparticle-mediated photothermal therapy: applications and opportunities for multimodal cancer treatment. Wiley Interdiscip Rev Nanomed Nanobiotechnol. 2017;9(4): e1449.
- [5] Rastinehad AR, Anastos H, Wajswol E, et al. Gold nanoshell-localized photothermal ablation of prostate tumors in a clinical pilot device study. Proc Natl Acad Sci U S A. 2019;116(37):18590– 18596. doi: 10.1073/pnas.1906929116.
- 6] Stern JM, Kibanov Solomonov VV, Sazykina E, et al. Initial evaluation of the safety of nanoshell-Directed photothermal therapy

- in the treatment of prostate disease. Int J Toxicol. 2016;35(1):38-46. doi: 10.1177/1091581815600170.
- Gad SC, Sharp KL, Montgomery C, et al. Evaluation of the toxicity of intravenous delivery of auroshell particles (gold-silica nanoshells). Int J Toxicol. 2012;31(6):584-594. doi: 10.1177/ 1091581812465969.
- Chen Z, Zhao P, Luo Z, et al. Cancer cell membrane—biomimetic [8] nanoparticles for homologous-targeting dual-modal imaging and photothermal therapy. ACS Nano. 2016;10(11):10049-10057. doi: 10.1021/acsnano.6b04695.
- Long Y, Wu X, Li Z, et al. PEGylated WS2 nanodrug system with erythrocyte membrane coating for chemo/photothermal therapy of cervical cancer. Biomater Sci. 2020;8(18):5088-5105. doi: 10. 1039/d0bm00972e.
- [10] Wang C, Wu B, Wu Y, et al. Camouflaging nanoparticles with brain metastatic tumor cell membranes: a new strategy to traverse blood-brain barrier for imaging and therapy of brain tumors. Adv Funct Mater. 2020;30(14):1909369.
- [11] Jia Y, Wang X, Hu D, et al. Phototheranostics: active targeting of orthotopic glioma using biomimetic proteolipid nanoparticles. ACS Nano. 2019;13(1):386-398. doi: 10.1021/acsnano.8b06556.
- Yang Q, Xiao Y, Yin Y, et al. Erythrocyte membrane-camouflaged IR780 and DTX coloading polymeric nanoparticles for imagingguided cancer photo-chemo combination therapy. Mol Pharm. 2019;16(7):3208-3220. doi: 10.1021/acs.molpharmaceut.9b00413.
- Lai J, Deng G, Sun Z, et al. Scaffolds biomimicking macrophages for a glioblastoma NIR-Ib imaging guided photothermal therapeutic strategy by crossing blood-brain barrier. Biomaterials. 2019;211:48-56. doi: 10.1016/j.biomaterials.2019.04.026.
- Geng X, Gao D, Hu D, et al. Active-targeting NIR-II phototheranostics in multiple tumor models using platelet-camouflaged nanoprobes. ACS Appl Mater Interfaces. 2020;12(50):55624-55637. doi: 10.1021/acsami.0c16872.
- [15] Li J, Zhen X, Lyu Y, et al. Cell membrane coated semiconducting polymer nanoparticles for enhanced multimodal cancer phototheranostics. ACS Nano. 2018;12(8):8520-8530. doi: 10.1021/acsnano.8b04066.
- [16] Zheng D, Yu P, Wei Z, et al. RBC membrane camouflaged semiconducting polymer nanoparticles for near-infrared photoacoustic imaging and photothermal therapy. Nano-Micro Lett. 2020;12(1): 94. doi: 10.1007/s40820-020-00429-x.
- [17] Huang X, Shang W, Deng H, et al. Clothing spiny nanoprobes against the mononuclear phagocyte system clearance in vivo: photoacoustic diagnosis and photothermal treatment of early stage liver cancer with erythrocyte membrane-camouflaged gold nanostars. Appl Mater Today. 2020;18:100484. doi: 10.1016/j. apmt.2019.100484.
- [18] Sun J, Wang J, Hu W, et al. Camouflaged gold nanodendrites enable synergistic photodynamic therapy and NIR biowindow II photothermal therapy and multimodal imaging. ACS Appl Mater Interfaces, 2021:13(9):10778-10795, doi: 10.1021/acsami.1c01238.
- Yu GT, Rao L, Wu H, et al. Myeloid-derived suppressor cell membrane-coated magnetic nanoparticles for cancer theranostics by inducing macrophage polarization and synergizing immunogenic cell death. Adv Funct Mater. 2018;28(37):1801389.
- [20] Rao L, Cai B, Bu LL, et al. Microfluidic electroporation-facilitated synthesis of erythrocyte membrane-coated magnetic nanoparticles for enhanced imaging-guided cancer therapy. ACS Nano. 2017;11(4):3496-3505. doi: 10.1021/acsnano.7b00133.
- [21] Lin K, Cao Y, Zheng D, et al. Facile phase transfer of hydrophobic Fe3O4@Cu2-XS nanoparticles by red blood cell membrane for MRI and phototherapy in the second near-Infrared window. J Mater Chem B. 2020;8(6):1202-1211. doi: 10.1039/c9tb02766a.
- [22] Ren X, Zheng R, Fang X, et al. Red blood cell membrane camouflaged magnetic nanoclusters for imaging-guided photothermal therapy. Biomaterials. 2016;92:13-24. doi: 10.1016/j.biomaterials.
- [23] Jiang Q, Luo Z, Men Y, et al. Red blood cell membrane-camouflaged melanin nanoparticles for enhanced photothermal therapy.

- Biomaterials. 2017;143:29-45. doi: 10.1016/j.biomaterials.2017.07.
- [24] Jiang Q, Liu Y, Guo R, et al. Erythrocyte-cancer hybrid membranecamouflaged melanin nanoparticles for enhancing photothermal therapy efficacy in tumors. Biomaterials. 2019;192:292-308. doi: 10.1016/i.biomaterials.2018.11.021.
- Wang D, Dong H, Li M, et al. Erythrocyte-cancer hybrid membrane camouflaged hollow copper sulfide nanoparticles for prolonged circulation life and homotypic-targeting photothermal/ chemotherapy of melanoma. ACS Nano. 2018;12(6):5241-5252. doi: 10.1021/acsnano.7b08355.
- Wang P, Kankala RK, Chen B, et al. Cancer cytomembrane-cloaked Prussian blue nanoparticles enhance the efficacy of mild-temperature photothermal therapy by disrupting mitochondrial functions of cancer cells. ACS Appl Mater Interfaces. 2021;13(31): 37563-37577. doi: 10.1021/acsami.1c11138.
- [27] Wang ZH, Liu JM, Zhao N, et al. Cancer cell macrophage membrane camouflaged persistent luminescent nanoparticles for imaging-guided photothermal therapy of colorectal cancer. ACS Appl Nano Mater. 2020;3(7):7105–7118. doi: 10.1021/acsanm. 0c01433
- Zhao H, Li L, Zhang J, et al. C-C chemokine ligand 2 (CCL2) recruits macrophage-membrane-camouflaged hollow bismuth selenide nanoparticles to facilitate photothermal sensitivity and inhibit lung metastasis of breast cancer. ACS Appl Mater Interfaces. 2018;10(37):31124-31135. doi: 10.1021/acsami. 8b11645.
- [29] Shen J, Karges J, Xiong K, et al. Cancer cell membrane camouflaged iridium complexes functionalized black-titanium nanoparticles for hierarchical-targeted synergistic NIR-II photothermal and sonodynamic therapy. Biomaterials. 2021;275:120979. doi: 10. 1016/i.biomaterials.2021.120979.
- Kelkar SS, Reineke TM. Theranostics: combining imaging and therapy. Bioconjugate Chem. 2011;22(10):1879–1903. [Database] doi: 10.1021/bc200151q.
- Blanco E, Shen H, Ferrari M. Principles of nanoparticle design for [31] overcoming biological barriers to drug delivery. Nat Biotechnol. 2015;33(9):941-951. doi: 10.1038/nbt.3330.
- [32] García-Álvarez R, Vallet-Regí M. Hard and soft protein corona of nanomaterials: analysis and relevance. Nanomaterials. 2021;11(4): 888. doi: 10.3390/nano11040888.
- Ke PC, Lin S, Parak WJ, et al. A decade of the protein corona. ACS Nano. 2017;11(12):11773-11776. doi: 10.1021/acsnano.7b08008.
- [34] Lundqvist M, Stigler J, Elia G, et al. Nanoparticle size and surface properties determine the protein corona with possible implications for biological impacts. Proc Natl Acad Sci U S A. 2008; 105(38):14265-14270. doi: 10.1073/pnas.0805135105.
- Verhoef JJF, Anchordoquy TJ. Questioning the use of PEGylation for drug delivery. Drug Deliv Transl Res. 2013;3(6):499-503. doi: 10.1007/s13346-013-0176-5.
- Thomas OS, Weber W. Overcoming physiological barriers to [36] nanoparticle delivery—are we there yet? Front Bioeng Biotechnol. 2019;7:415. doi: 10.3389/fbioe.2019.00415.
- [37] Valcourt DM, Harris J, Riley RS, et al. Advances in targeted nanotherapeutics: from bioconjugation to biomimicry. Nano Res. 2018; 11(10):4999-5016. doi: 10.1007/s12274-018-2083-z.
- [38] Dai Q, Wilhelm S, Ding D, et al. Quantifying the ligand-coated nanoparticle delivery to cancer cells in solid tumors. ACS Nano. 2018;12(8):8423-8435. doi: 10.1021/acsnano.8b03900.
- [39] Hu C-MJ, Zhang L, Aryal S, et al. Erythrocyte membrane-camouflaged polymeric nanoparticles as a biomimetic delivery platform. Proc Natl Acad Sci U S A. 2011;108(27):10980-10985. doi: 10. 1073/pnas.1106634108.
- [40] Harris JC, Scully MA, Day ES. Cancer cell membrane-coated nanoparticles for cancer management. Cancers. 2019;11(12):1836. doi: 10.3390/cancers11121836.
- Liao Y, Zhang Y, Blum NT, et al. Biomimetic hybrid membrane-[41] based nanoplatforms: synthesis, properties and biomedical applications. Nanoscale Horiz. 2020;5(9):1293-1302. doi: 10.1039/ d0nh00267d.



- [42] Scully MA, Sterin EH, Day ES. Membrane-wrapped nanoparticles for nucleic acid delivery, biomater. Biomater Sci. 2022;10(16): 4378-4391. doi: 10.1039/d2bm00447j.
- [43] Aboeleneen SB, Scully MA, Harris JC, et al. Membrane-wrapped nanoparticles for photothermal cancer therapy. Nano Converg. 2022-9-37
- [44] Zhu JY, Zheng DW, Zhang MK, et al. Preferential cancer cell selfrecognition and tumor self-targeting by coating nanoparticles with homotypic cancer cell membranes. Nano Lett. 2016;16(9): 5895-5901. doi: 10.1021/acs.nanolett.6b02786.
- Heimburg J, Yan J, Morey S, et al. Inhibition of spontaneous breast cancer metastasis by anti-Thomsen-Friedenreich antigen monoclonal antibody JAA-F11. Neoplasia. 2006;8(11):939-948. doi: 10.1593/neo.06493.
- [46] Liu L, Bai X, Martikainen MV, et al. Cell membrane coating integrity affects the internalization mechanism of biomimetic nanoparticles. Nat Commun. 2021;12(1):5726. doi: 10.1038/s41467-021-
- [47] Li S, Jiang W, Yuan Y, et al. Delicately designed cancer cell membrane-camouflaged nanoparticles for targeted 19F MR/PA/FL imaging-guided photothermal therapy. ACS Appl Mater Interfaces. 2020;12(51):57290-57301. doi: 10.1021/acsami.0c13865.
- [48] Estelrich J, Sánchez-Martín MJ, Busquets MA. Nanoparticles in magnetic resonance imaging: from simple to dual contrast agents. Int J Nanomed. 2015;10:1727-1741. doi: 10.2147/IJN. S76501.
- [49] Rich LJ, Chamberlain SR, Falcone DR, et al. Performance characteristics of photoacoustic imaging probes with varying frequencies and light-delivery schemes, ultrason. Ultrason Imaging. 2019; 41(6):319-335. doi: 10.1177/0161734619879043.
- [50] Chen B, Dai W, Mei D, et al. Comprehensively priming the tumor microenvironment by cancer-associated fibroblast-targeted liposomes for combined therapy with cancer cell-targeted chemotherapeutic drug delivery system. J Control Release. 2016;241:68-80. doi: 10.1016/j.jconrel.2016.09.014.
- [51] Mu X, Li J, Yan S, et al. SiRNA delivery with stem cell membranecoated magnetic nanoparticles for imaging-guided photothermal

- therapy and gene therapy. ACS Biomater Sci Eng. 2018;4(11): 3895-3905. doi: 10.1021/acsbiomaterials.8b00858.
- [52] Chen Y, Zhao G, Wang S, et al. Platelet-membrane-camouflaged bismuth sulfide nanorods for synergistic radio-photothermal therapy against cancer. Biomater Sci. 2019;7(8):3450-3459. doi: 10. 1039/c9bm00599d.
- [53] Ren X, Yang S, Yu N, et al. Cell membrane camouflaged bismuth nanoparticles for targeted photothermal therapy of homotypic tumors. J Colloid Interface Sci. 2021;591:229-238. doi: 10.1016/j. icis.2021.02.006.
- [54] Zhen X, Cheng P, Pu K. Recent advances in cell membrane-camouflaged nanoparticles for cancer phototherapy. Small. 2019; 15(1):e1804105. doi: 10.1002/smll.201804105.
- [55] Yi X, Duan Q-Y, Wu F-G. Low-temperature photothermal therapy: strategies and applications. Research. 2021;2021:9816594. doi: 10. 34133/2021/9816594.
- Ye S, Wang F, Fan Z, et al. Light/PH-triggered biomimetic red blood cell membranes camouflaged small molecular drug assemblies for imaging-guided combinational chemo-photothermal therapy. ACS Appl Mater Interfaces. 2019;11(17):15262-15275. doi: 10.1021/acsami.9b00897.
- Fay BL, Melamed JR, Day ES. Nanoshell-mediated photothermal therapy can enhance chemotherapy in inflammatory breast cancer cells. Int J Nanomed. 2015;10:6931-6941. doi: 10.2147/IJN. S93031.
- Frey B, Weiss EM, Rubner Y, et al. Old and new facts about hyper-[58] thermia-induced modulations of the immune system. Int J Hyperthermia. 2012;28(6):528-542. doi: 10.3109/02656736.2012. 677933.
- [59] Sun J, Zhao H, Xu W, et al. Recent advances in photothermal therapy-based multifunctional nanoplatforms for breast cancer. Front Chem. 2022;10:1024177. doi: 10.3389/fchem.2022.1024177.
- [60] Albanese A, Tang PS, Chan WCW. The effect of nanoparticle size, shape, and surface chemistry on biological systems. Annu Rev Biomed Eng. 2012;14(1):1-16. doi: 10.1146/annurev-bioeng-071811-150124.